

# **Effect of the Wall Tilt on the Optical Properties of Integrated Directional Couplers**

**A. Llobera<sup>1</sup>, I. Salinas<sup>2</sup>, I. Garcés<sup>3</sup>, A. Merlos<sup>1</sup> and C. Domínguez<sup>1</sup>**

1. CNM-CSIC. Departament de Tecnologia de Silici. Campus UAB 08193 Barcelona, Spain

2. Departamento de Física Aplicada, Universidad de Zaragoza, 50009 Zaragoza, Spain

3. Depart. Ingeniería Elect. y Com., Universidad de Zaragoza, 50015 Zaragoza, Spain

The effect of the wall tilt on the performance of directional couplers has been studied. Results show that there is a significant reduction of the coupling length as the tilt decreases when non-vertical walls, which are inherent in nearly all Clean Room waveguide fabrication processes, are considered. Comparing coupling lengths of 90° and 45°, it has been observed how there nearly exists a 2 factor between them. Experimental data obtained with ARROW-B directional couplers confirm that tilt effects should be considered in any device with large core thickness. © 2001 Optical Society of America

*Ocis codes: 130.0130, 230.0230, 230.3120, 230.7370*

## **Introduction**

Directional couplers are used in a wide variety of applications, such as filters, WDM and polarisation splitters<sup>1</sup>. A directional coupler normally consists on two identical single-mode waveguides placed in close proximity so as to allow coupling between the evanescent fields. Using Coupled-Mode Theory<sup>2</sup>, the coupling length can be defined as the distance required for maximum energy transference, and can be written as  $L_{c0}=\pi/(\beta_s-\beta_a)$ , where  $\beta_s$  and  $\beta_a$  are the propagation constants of the symmetric and antisymmetric modes of the parallel coupled structure.

Simulations of integrated optical devices are commonly done assuming 90° tilt (vertical) waveguide walls. Although this approximation generally gives good results, when considering directional couplers there exists a mismatch between simulation and experimental data. The tilt on the waveguide walls is inherent on every etching process: wet etching provide, for an amorphous material, 45° tilt walls, which significantly reduce the light confinement and increase its attenuation as compared to 90° tilt walls. It is feasible to obtain higher tilts using dry etching processes. Depending on the etching conditions, the tilt could vary from the same values of the wet etching to 90° tilt. It has to be noted, however, that the etching conditions for this latter tilt value are extremely aggressive and the layers frequently suffer an overetching or a non-uniform etching during this process. In our case, using Reactive Ion Etching (RIE) with the working conditions optimised, it was possible to obtain 80° tilt walls on silicon oxide, with low roughness, as shown in fig. 1.

The wall tilt in integrated optics devices should be taken into account if large core thicknesses are considered, since its optical properties could be significantly distorted from the ideal case of vertical walls. As an example of large core thickness device, the effects of the non-vertical walls have been studied for an ARROW-B directional coupler. It has to be noted, however, that the

effects of the wall tilt not only are restricted to ARROW configuration but also are present in any device based on Total Internal Reflection with small refractive index difference between the core and the surrounding layers.

Antiresonant Reflecting Optical Waveguides (ARROW) have recently received much attention due to their interesting properties<sup>3,4</sup>: optical confinement in the orthogonal direction of the layers is obtained via the very high reflectivity of a Fabry-Perot structure placed beneath the core. This interference cladding provides its single-mode behaviour at the working wavelength for a given core thickness. The whole structure can also be designed to be polarisation-selective or non-selective, being the latter called ARROW-B<sup>5</sup>. The ARROW-B refractive index profile and the directional coupler structure can be seen in fig.2. The guiding properties as function of the 1<sup>st</sup> and 2<sup>nd</sup> cladding ( $d_1$  and  $d_2$ ) have previously been analysed by other authors<sup>6</sup>. Minimum attenuation losses are obtained when the second cladding is half of the core. It also has been shown<sup>7</sup> that ARROW-B, due to its layer configuration, are less polarisation dependent as compared to other types of ARROW structures.

In all the following discussion, the axis will be as shown in fig. 2: x and y will be the horizontal and vertical cross-section coordinates, respectively, and z will stand for the longitudinal (or propagation) axis.

In order to introduce the effect of non-vertical walls in the simulations, the commercially available finite-element ANSYS® 5.7 in University version has been used. The evolution of the intensity profile with z has been done using home-made computational program based on Non-Uniform Finite Difference Method (NU-FDM)<sup>8</sup> and the Beam Propagation Method (BPM)<sup>9</sup>, together with the Effective Index Method (EIM)<sup>10</sup>, to reduce the dimensions of the structure.

## **Fabrication**

10 ARROW-B directional couplers were fabricated using fully compatible silicon CMOS process, each one with different  $L_{co}$ , ranging from 1 to 10 mm. All ARROW-B layers were obtained by deposition of non-stoichiometric silicon oxide ( $SiO_x$ ) using a parallel plate PLASMALAB 80+ Plasma Enhanced Chemical Vapour Deposition (PECVD) system, working at 300°C, 200mTorr and 30Watt. Layers deposited by PECVD using pure silane ( $SiH_4$ ) and nitrous oxide ( $N_2O$ ) as precursors are suggested to have different stoichiometries depending on the gas flow ratio, which modifies the refractive index of the layer between 1.46 and 1.9, as previously described<sup>11</sup>.

The ARROW multilayer devices were obtained by deposition onto the P-doped (100) silicon wafer substrate (refractive index  $n=3.85+0.02i$  at 633nm). Three layers compose this structure:

Second cladding layer: 2 $\mu$ m silicon oxide ( $n_2=1.54$ )

First cladding layer: 0.3 $\mu$ m silicon oxide ( $n_1=1.46$ )

Core: 4 $\mu$ m silicon oxide ( $n_c=1.54$ )

In order to obtain horizontal directional couplers, the core was 1.5 $\mu$ m etched by RIE. Simulations with  $w=5\mu$ m and  $d_0=2\mu$ m provided good light confinement and a relative short coupling length when considering the case of 90° wall tilt.

## Results

The symmetric and antisymmetric mode profiles of the ARROW-B directional coupler were studied, together with its dependence on the tilt angle. As can be seen in fig 3, the decrease in the tilt angle causes a modification of the first directional coupler modes: The broadening of the symmetrical mode and the slight separation of the lobes of the antisymmetrical mode. This variation can be clearly understood if the AA' cut is done on the contour plots and the coupling length as function of the tilt angle is studied, as is shown in figures 4 and 5. At high tilts, the

waveguides have a strong confinement factor. Hence, the evanescent field is the lowest and, as a consequence, the coupling length has a maximum value. As the tilt decreases, the field adapts its profile to the waveguide morphology and the modes are not so strong confined, increasing the overlap between the evanescent field of the waveguides. The increasing difference between the effective index of the symmetric and antisymmetric mode causes an increase of the coupling constant ( $\kappa$ ) and thus, the coupling length decreases with the wall tilt, as also shown in fig. 5. It can be observed how there nearly exists a 100% difference in the coupling length of two identical directional couplers if their wall tilt differ  $45^\circ$ .

Measures of the directional couplers were done using a standard end-fire coupling system using a He-Ne laser working at  $\lambda=632.8$  nm. As can be seen in fig.6, when vertical walls ( $90^\circ$  tilt) are considered, experimental and simulation results do not match, since the coupling length has a higher value than predicted. When the technological results are considered, that is, if the  $80^\circ$  wall tilt is introduced into simulations instead of perfectly vertical walls, a better matching is achieved, confirming that the deviations of the experimental results as compared to simulations were produced during the rib definition.

## **Conclusions**

The response of the directional coupler as function of the propagation distance ( $z$ ) has a periodical behaviour, as predicted both in theory and simulations. However, a significant mismatch between experimental and simulated value of the coupling length is obtained when perfect vertical walls are considered. This fact can be explained considering that the etching processes generally do not give perfectly vertical walls, but a certain tilt is always obtained. This tilt is responsible of the degree of the confinement in the waveguide. It also has been observed how the coupling length significantly depends on the wall tilt, since the decrease in the

confinement causes an enhancement of the coupling constant, which reduces the coupling length for 45° tilt walls, as compared to 90° walls, by a factor of 2. Results provided by the ARROW-B directional couplers confirms that if the integrated devices have a large core thickness, wall tilt should always be considered when studying its behaviour.

## Acknowledgements

A. Llobera thanks the Generalitat de Catalunya (Catalan council) for his grant (2001-TDOC-00008)

## References

1. S.Asakawa and A. R. Mickelson. “Dual-Wavelength ( $\lambda=1300-1650\text{nm}$ ) Directional Coupler Multiplexer-Demultiplexer by the annealed-proton-exchange process in  $\text{LiNbO}_3$ ”. *Optics Lett.* **18**(6), 417-419 (1993).
2. H.Haus and W. Huang. “Coupled-mode Theory”. *Proc.IEEE* **79**(10), 1505-1518 (1991).
3. T.Baba and Y. Kokubun. “Dispersion and Radiation Loss Characteristics of Antiresonant Reflecting Optical Waveguides-Numerical Results and Analytical Expressions”. *Jour.Quant.Elect.* **28**(7), 1689-1700 (1992).
4. I.Garcés, F. Villuendas J. A. Vallés C. Domínguez and M. Moreno. “Analysis of Leakage Properties and Guiding Conditions of Rib Antiresonant Reflecting Optical Waveguides”. *Jour.Light.Tech.* **14**(5), 798-805 (1996).
5. T.Baba and Y. Kokubun. “New Polarization-Insensitive Antiresonant Reflecting Optical Waveguide (ARROW-B)”. *Phot.Tech.Lett.* **1**(8), 232-234 (1989).
6. W.Huang, R. Shubair A. Nathan and Y. L. Chow. “The Modal Characteristics of ARROW Structures”. *Jour.Light.Tech.* **10**(8), 1015-1022 (1992).

7. T. Baba and Y. Kokubun “Dispersion and Radiation Loss Characteristics of Antiresonant Reflecting Optical Waveguides- Numerical Results and Analytical Expressions”, Jour. Quant. Elect. **28**(7), 1689-1700 (1992).
8. C.Kim and R. Ramaswamy. “Modelling of Graded-Index Channel Waveguides Using Nonuniform Finite Difference Method”. Jour.Light.Tech. **7**(10), 1581-1589 (1989).
9. Y.Chung and N. Dagli. “Analysis of Z-Invariant and Z-Variant Semiconductor Rib Waveguides by Explicit Finite Difference Beam propagation Method with Nonuniform Mesh Configuration”. Jour.Quantum.Elect. **27**(10), 2296-2305 (1991).
10. R.Knox and P. Toullos. “Integrated Circuits for the Millimeter Optical Frequency Range”. Proc.Symp.Submillimetre Waves (Polytechnic Press), 497-516 (1970).
11. C.Domínguez, J. A. Rodríguez F. Muñoz and N. Zine. “Plasma Enhanced CVD Silicon Oxide Films for Integrated Optics Applications”. Vacum **52**, 395-400 (1999).

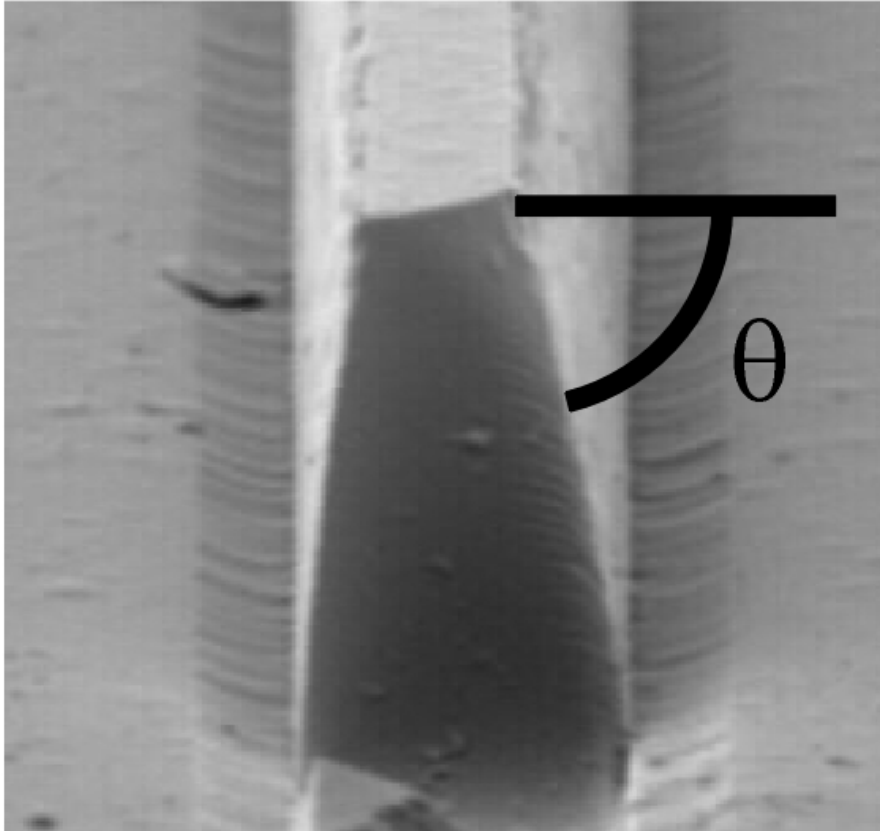


FIGURE 1



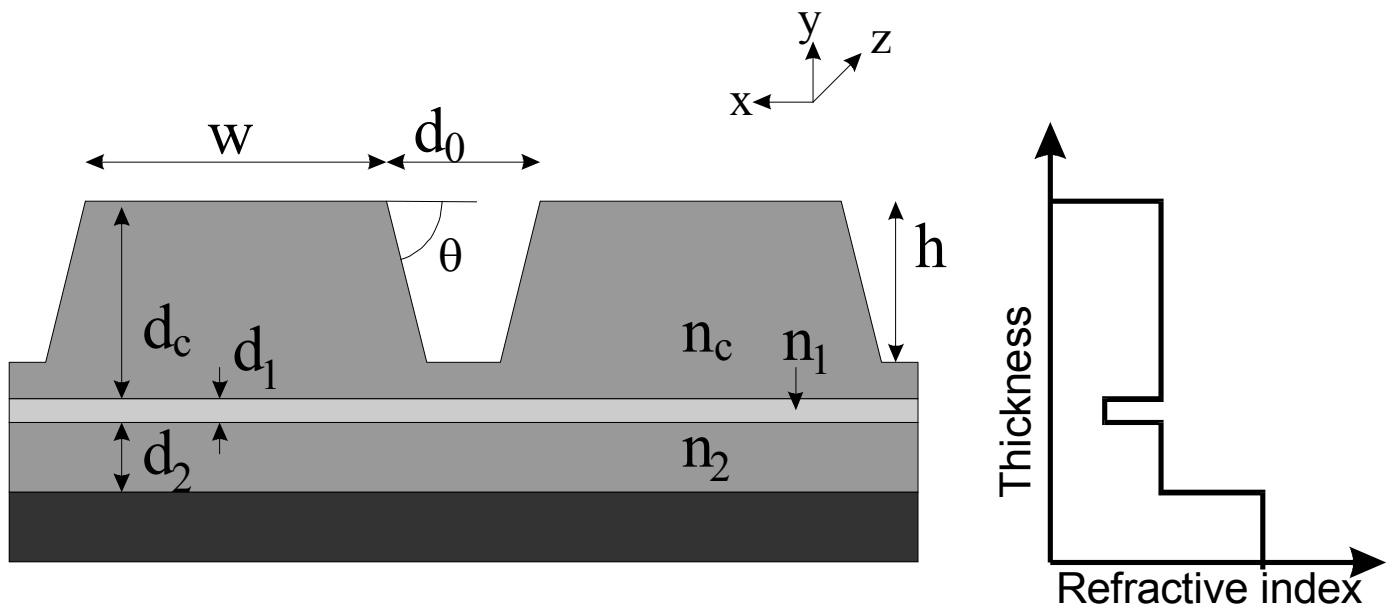


FIGURE 2



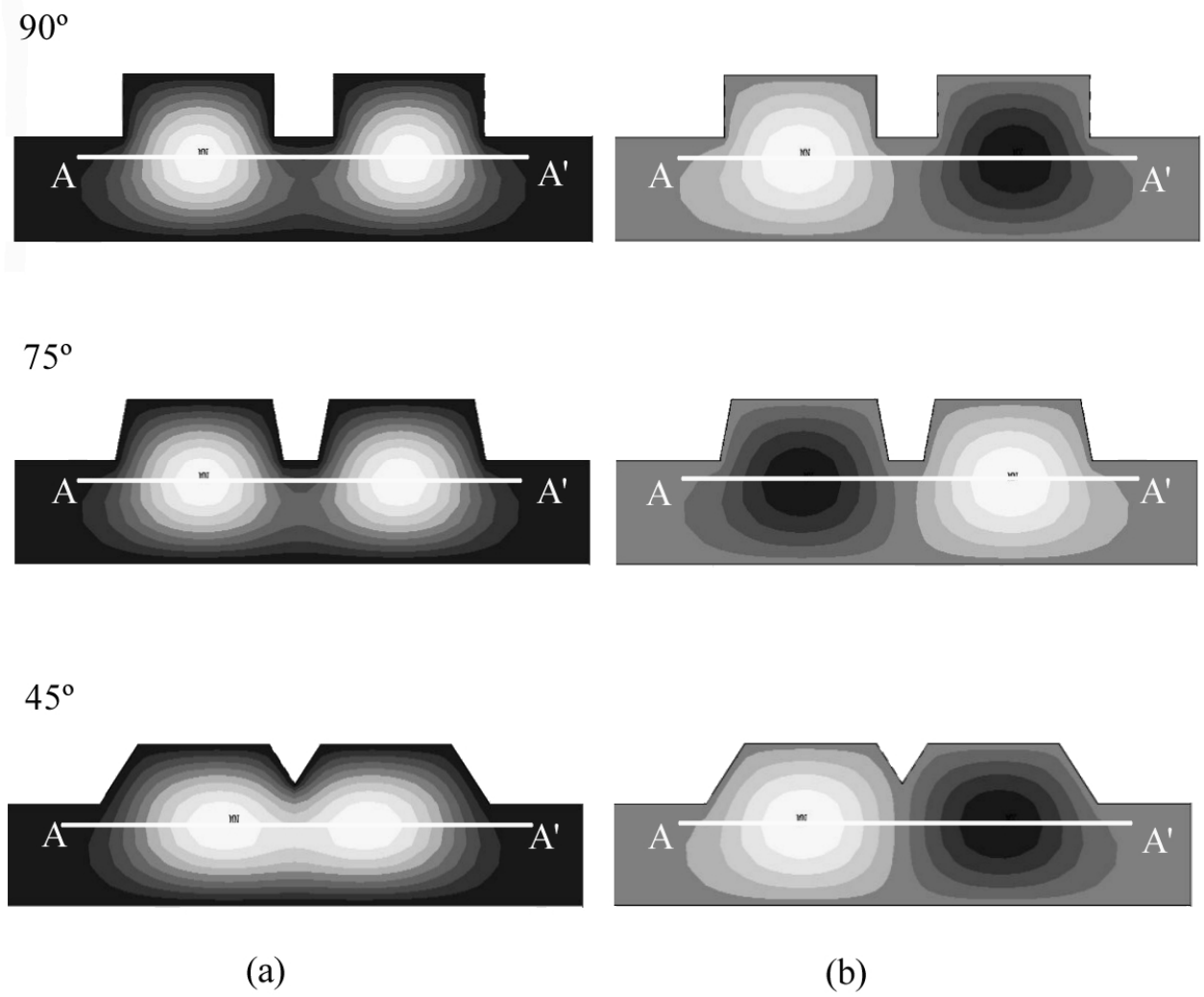


FIGURE 3

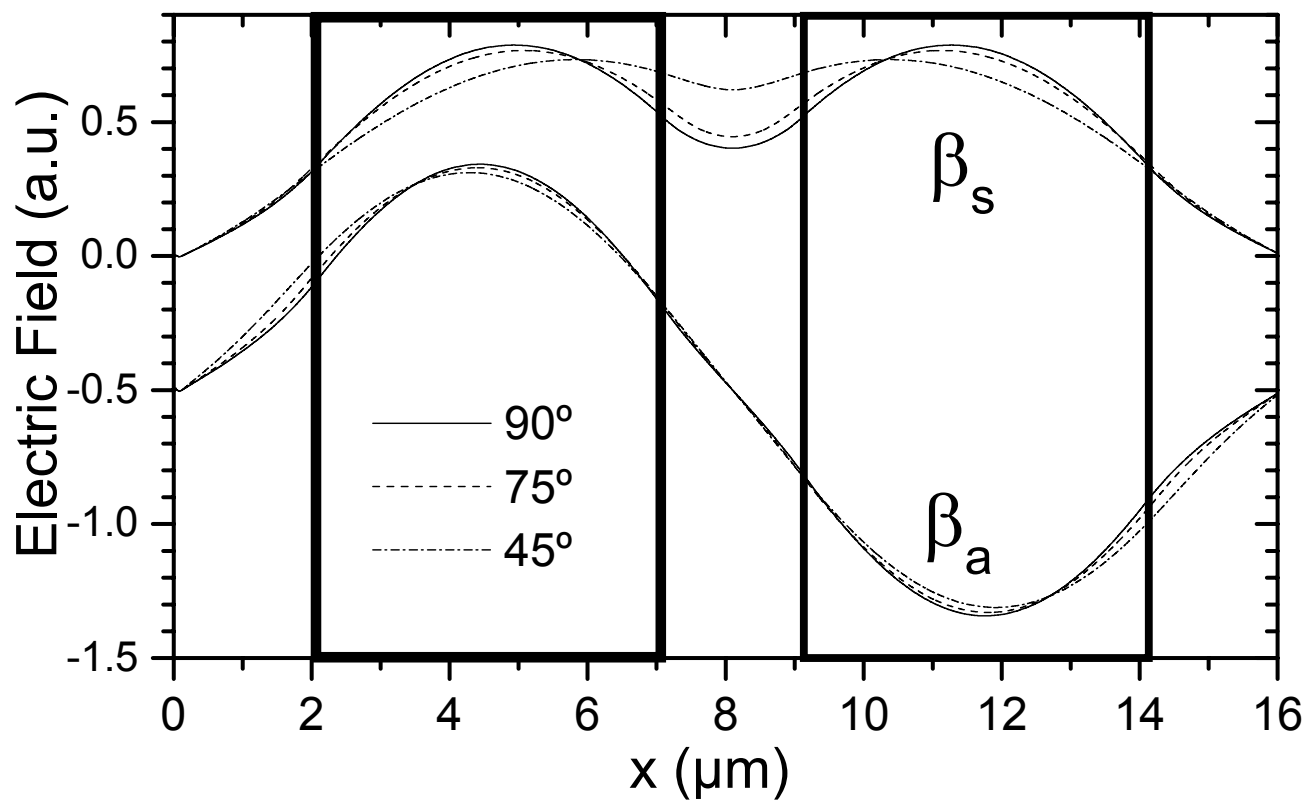


FIGURE 4

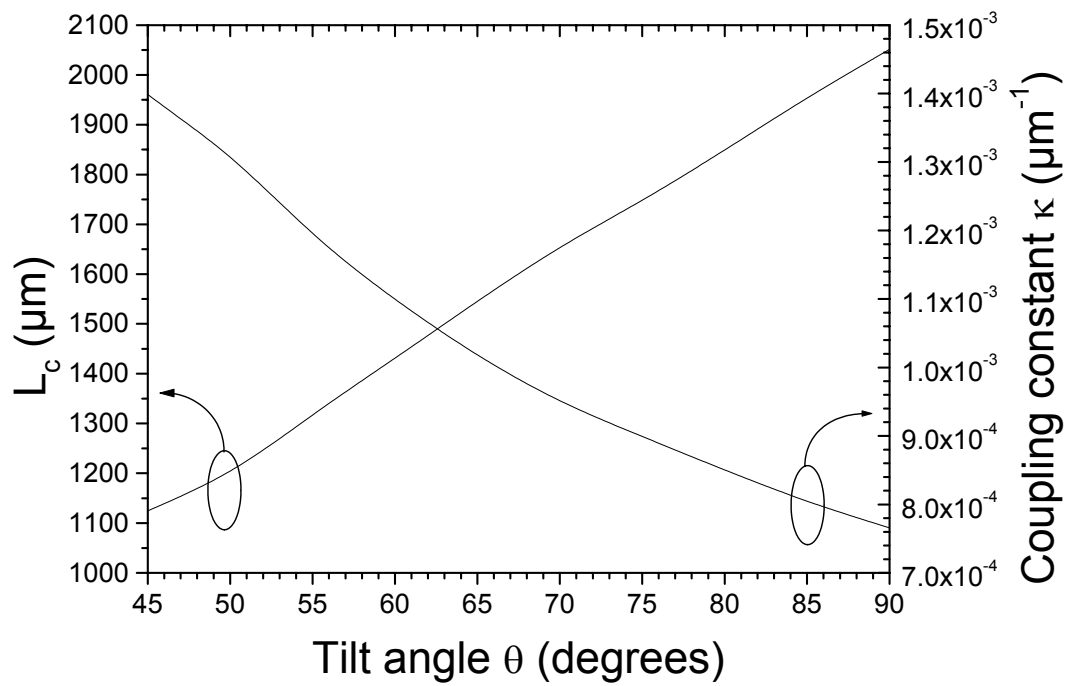
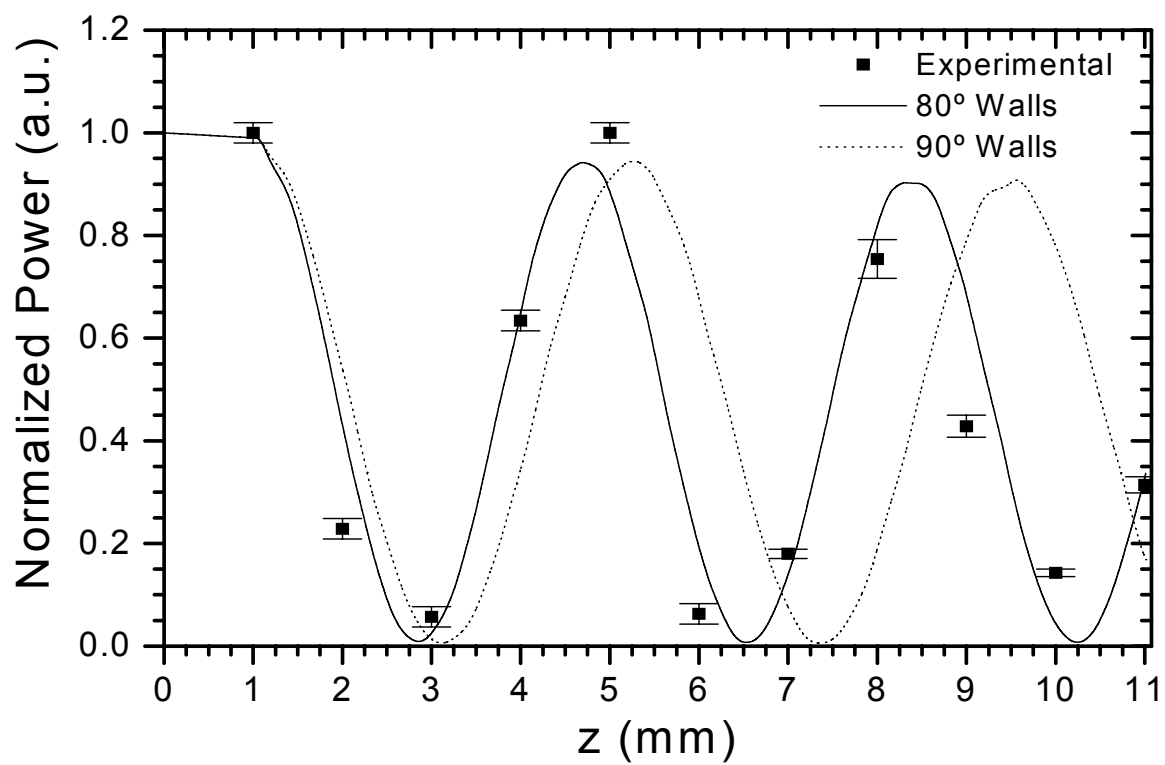


FIGURE 5



## FIGURE 6

**Fig. 1:** SEM microphotograph of the core of a  $2\mu\text{m}$ -width,  $3.5\mu\text{m}$ -rib waveguide, where the wall tilt due to RIE process can be observed.

**Fig. 2:** Fundamental structure and refractive index profile of ARROW-B directional couplers.

**Fig. 3:** Electric Field profile of the symmetric and antisymmetric modes in an ARROW-B directional coupler, for 3 different wall tilt. ~~Lateral size of waveguides has been cut in order to show better the effect at the walls.~~

**Fig. 4:** AA' cut of the symmetric and antisymmetric modes of fig, 3, where the increasing evanescent field overlap of the symmetric mode can be observed, together with the lobe separation of the antisymmetric mode.

**Fig. 5:** Coupling length and effective index difference as function of the tilt angle



**fig. 6:** Power interchange between ARROW-B waveguides of the Directional Coupler as function of the distance: Experimental, Simulation with vertical rib and Simulation with 80° tilted rib.